Increased ER Stress After Experimental Ischemic Optic Neuropathy and Improved RGC and Oligodendrocyte Survival After Treatment With Chemical Chaperon

Varun Kumar,*[,1] Louise Alessandra Mesentier-Louro,[1] Angela Jinsook Oh,[1] Kathleen Heng,[1] Mohammad Ali Shariati,[1] Haoliang Huang,[1] Yang Hu,[1] and Yaping Joyce Liao[1,2]

[1]Department of Ophthalmology, Stanford University, School of Medicine, Stanford, California, United States
[2]Department of Neurology, Stanford University, School of Medicine, Stanford, California, United States

Correspondence: Yaping Joyce Liao, Department of Ophthalmology, Stanford University Medical Center, 2452 Watson Court, Palo Alto, CA 94303-5353, USA; yjliao@stanford.edu.

Current affiliation: *Department of Ophthalmology, Harvard Medical School, Cambridge, Massachusetts, United States.

Submitted: May 23, 2018
Accepted: February 12, 2019

Citation: Kumar V, Mesentier-Louro LA, Oh AJ, et al. Increased ER stress after experimental ischemic optic neuropathy and improved RGC and oligodendrocyte survival after treatment with chemical chaperon. *Invest Ophthalmol Vis Sci*. 2019;60:1953–1966. https://doi.org/10.1167/iovs.18-24890

Purpose. Increased endoplasmic reticulum (ER) stress is one of the earliest subcellular changes in neuro-ophthalmic diseases. In this study, we investigated the expression of key molecules in the ER stress pathways following nonarteritic anterior ischemic optic neuropathy (AION), the most common acute optic neuropathy in adults over 50, and assessed the impact of chemical chaperon 4-phenylbutyric acid (4-PBA) in vivo.

Methods. We induced AION using photochemical thrombosis in adult mice and performed histologic analyses of key molecules in the ER stress pathway in the retina and optic nerve. We also assessed the effects of daily intraperitoneal injections of 4-PBA after AION.

Results. In the retina at baseline, there was low proapoptotic transcriptional regulator C/EBP homologous protein (CHOP) and high prosurvival chaperon glucose-regulated protein 78 (GRP78) expression in retinal ganglion cells (RGCs). One day after AION, there was significantly increased CHOP and reduced GRP78 expressions in the ganglion cell layer. In the optic nerve at baseline, there was little CHOP and high GRP78 expression. One day after AION, there was significantly increased CHOP and no change in GRP78 expression. Treatment immediately after AION using daily intraperitoneal injection of chemical chaperone 4-PBA for 19 days significantly rescued Brn3A$^+$ RGCs and Olig2$^+$ optic nerve oligodendrocytes.

Conclusions. We showed for the first time that acute AION resulted in increased ER stress and differential expression of ER stress markers CHOP and GRP78 in the retina and optic nerve. Rescue of RGCs and oligodendrocytes with 4-PBA provides support for ER stress reduction as possible treatment for AION.

Keywords: endoplasmic reticulum, ER stress, metabolic stress, AION, OCT, retinal ganglion cell, optic neuropathy, chaperon, unfolded protein response, 4-phenylbutyric acid

Nonarteritic anterior ischemic optic neuropathy (AION) is the most common acute optic neuropathy in those greater than 50 years old.[1–3] Patients with nonarteritic AION typically present with painless, sudden vision loss involving half or more of the visual field in one eye, and there is a 25% risk of contralateral eye involvement.[4] In human AION, ischemia occurs initially posterior to the lamina cribrosa, in the posterior ciliary artery territory,[2,3,5] involving the unmyelinated and the anterior, myelinated portions of the optic nerve.

In photochemical thrombosis rodent models of AION, we know that within 24 hours after ischemia, there is severe optic nerve head edema and swelling[6–13] as well as abnormal visual evoked potential responses.[6,8,11] Acutely, there is also prominent microglial activation and postischemic inflammatory response.[6,7,12,14] By week 1, there is massive degeneration of retinal ganglion cell (RGC) axons, prominent loss of CNPase$^+$ optic nerve oligodendrocytes, and anterograde optic nerve demyelination.[6,7,11,15] By week 3, there is relatively stable, irreversible thinning of the retina, loss of Brn3A$^+$ RGCs and optic nerve oligodendrocytes per optical coherence tomography (OCT) and histology.[6–9,11,15–18] The severity of the acute retinal swelling correlated with that of the chronic thinning and RGC loss.[19] Unfortunately, there is currently no effective treatment for AION.

A promising therapeutic target in the treatment of vision loss due to optic neuropathies is the unfolded protein response (UPR) pathway, an endogenous and early line of defense against many different types of injury.[20,21] Early after insult, the prosurvival pathway is activated, including activation of the master endoplasmic reticulum (ER) chaperon glucose-regulated protein 78 (GRP78), also known as the immunoglobulin heavy chain-binding protein (BiP) or heat shock protein (HSP) A5.[20,22] GRP78 helps to translocate newly synthesized polypeptides across the ER membrane, facilitate the folding and assembly of proteins, target misfolded proteins for ER-associated degradation (ERAD), regulate calcium homeostasis, and serve as an ER stress sensor.[23] These adaptive responses help return cells to homeostasis.[20,21,24] In contrast, prolonged ER stress leads to activation of the proapoptotic pathway, including increased expression of the UPR-regulated proapoptotic transcription factor CCAAT/enhancer-binding protein (C/EBP) homologous protein (CHOP) and activation of the PERK-eIF2α-ATF4-CHOP

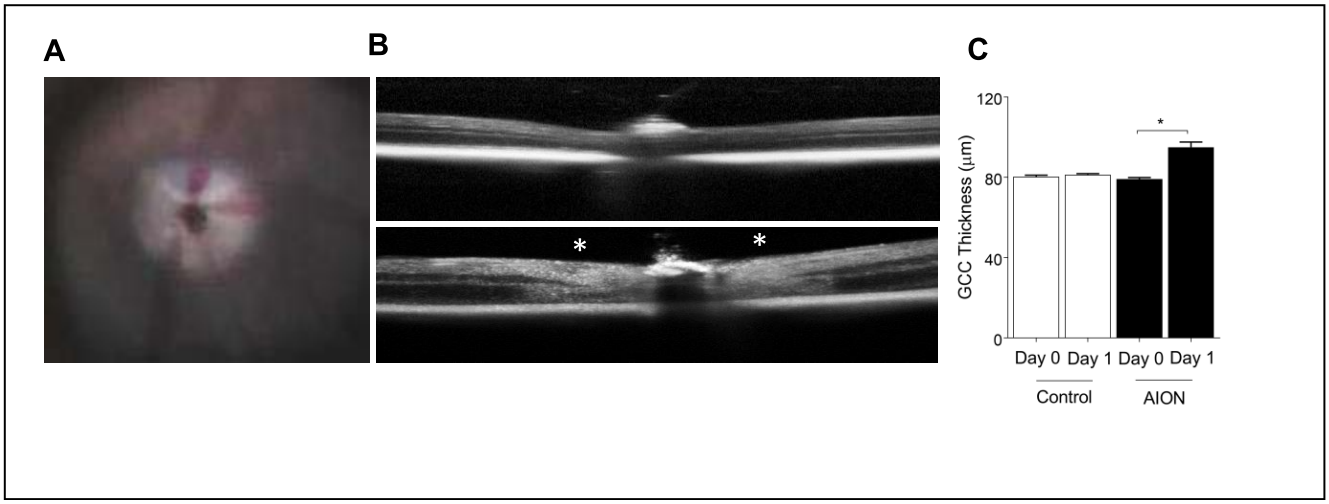

Figure 1. Photochemical thrombosis model of AION. (**A**) Mouse fundus photography immediately after AION showing whitening of optic nerve head due to ischemia. (**B**) Representative images of OCT line scan through optic disc of control (*top*) and AION (*bottom*) eyes 1 day after AION. Swelling around the optic nerve head is indicated by *white asterisks*. (**C**) Bar graph showing OCT GCC thickness measurements in control and AION eyes at day 0 and 1 ($n = 6$, $^*P = 0.0001$, 1-way ANOVA with Tukey multiple comparisons test). AION, anterior ischemic optic neuropathy; GCC, ganglion cell complex; OCT, optical coherence tomography.

pathway, leading to activation of proapoptotic genes *DR5*, *TRB3*, *BIM,* and *PUMA* and decrease in the expression of *BCL2*, which triggers apoptosis.[23,25,26] Increased ATF4-CHOP heterodimers also restores translation, leading to increased protein synthesis and further worsening of ER stress, ATP depletion, oxidative stress, activation of the inflammatory pathways, and cell death.[21,26,27]

The UPR pathway is important in many diseases that affect vision, including optic neuropathies.[28] Increased ER stress has been described in animal models of vision loss,[29,30] including in glaucoma,[31,32] optic nerve crush,[32,33] diabetic retinopathy,[34,35] hyperglycemia,[36,37] N-methyl-D-aspartate (NMDA)-induced RGC loss,[38] retinitis pigmentosa, experimental autoimmune encephalomyelitis (EAE),[39] and central nervous system (CNS) ischemia or reperfusion injury.[40–44] RNA sequencing (RNAseq) analysis of transcriptome profile 2 days following optic nerve crush in adult C57BL/6 mice showed that among the 177 differentially expressed genes, the ER stress-related gene *ATF4* and its transactivated downstream gene *CHOP* were particularly significantly upregulated.[45] Deletion of the proapoptotic molecule CHOP has been shown to improve RGC survival after ischemia-reperfusion injury,[41–43] optic nerve crush,[32,33] experimental glaucoma,[31,32] and EAE.[39]

Other than retinal neurons, increased ER stress is also important in diseases involving CNS glia, including in optic nerve oligodendrocytes, which exhibit selective vulnerability in hypoxic-ischemic injury due to their glutamate receptor expression.[46] CHOP upregulation is detected in oligodendrocytes after NMDA-induced retinal injury[38] and hypoxia.[47] CHOP upregulation is found in retinal astrocytes in DBA/2J glaucoma model[48] and after retina ischemia.[49,50] Other than blinding diseases, increased ER stress has been shown to play a role in different neurological conditions such as stroke,[40] Alzheimer's disease,[51] Parkinson's disease,[52] amyotrophic lateral sclerosis,[53,54] spinal cord injury,[40,55] and multiple sclerosis.[56]

Treatment aimed to reduce ER stress using chemical chaperon 4-phenylbutyric acid (4-PBA)[57–64] has been used to treat cystic fibrosis and liver injury. 4-PBA has been tested in animal models of vision loss and has shown to be protective in EAE[65] and glaucoma,[63] even as an eye drop.[62,64] There is also promising benefit of 4-PBA in animal models of stroke,[60,66] spinal cord ischemia,[59] and cardiac ischemic-reperfusion injury.[67–69] However, in one study of retinal ischemia (via high intraocular pressure), 4-PBA given prior to ischemia rescued 100% of RGCs, while treatment after ischemia showed no effect.[57] Other than neurons, there is also evidence that 4-PBA may act on glia. In a study of middle cerebral artery occlusion in rat, 4-PBA had a significant impact on the level of astrogliosis, which affected neuronal survival after stroke.[70] Also, 4-PBA treatment is associated with reduction of nitric oxide synthase and TNFα and may have a role in dampening postischemic inflammation and glial function.[66]

In this study, we used the well-established photochemical thrombosis model of AION to examine the expression patterns of key molecules important in ER stress acutely after optic nerve ischemia and determine the effects of chemical chaperon 4-PBA on RGCs and optic nerve glia after AION.

Materials and Methods

Animals

Adult male and female C57BL/6 mice (Charles River, Hollister, CA, USA) were kept at constant temperature, with a 12-hour light/dark cycle and food and water available ad libitum. We performed all animal care and experiments in accordance with the ARVO Statement for the Use of Animals in Ophthalmic and Vision Research, with approval from the Stanford University Administrative Panel on Laboratory Animal Care (APLAC). We did not address differences in sex as a biological variable. All procedures were performed under sedation with brief exposure to isoflurane followed by intraperitoneal injection of ketamine 50 to 100 mg/kg (Hospira, Inc., Lake Forest, IL, USA) and xylazine 2 to 5 mg/kg (Bedford Laboratories, Bedford, OH, USA). When necessary, the pupils of anesthetized mice were pharmacologically dilated with 1% tropicamide (Alcon Laboratories, Inc., Fort Worth, TX, USA) and 2.5% phenylephrine hydrochloride (Akorn, Inc., Lake Forest, IL, USA). All animals underwent serial manipulations (e.g., ischemia induction, repeat optical imaging measurements; see Fig. 1A), and were sacrificed for histological analyses.

Investigative Ophthalmology & Visual Science

Photochemical Thrombosis Model of AION

Following injection of rose bengal (1.25 mM in phosphate-buffered saline [PBS], 5 μL/g body weight) in tail vein, we induced AION in adult mice using photochemical thrombosis[9,71,72] with low energy transpupillary laser light spots (400 μm spot diameter, 50 mW power, 1-second duration, 15 spots) using a frequency doubled Nd:YAG laser (PASCAL; OptiMedica, Santa Clara, CA, USA). To ensure consistency, AION induction for all experiments in this study was performed by one person. Also, to improve rigor and reproducibility, we consistently induced AION in one eye and used the contralateral eye as control.

OCT and Segmentation

To measure retinal structural changes over time, we performed spectral-domain OCT analysis using Spectralis HRA+OCT instrument (Heidelberg Engineering, GmbH, Heidelberg, Germany).[9,71,72] We used the circular "retinal nerve fiber layer" ("RNFL") scans, and manually segmented the thickness of the ganglion cell complex (GCC) as described previously.[73,74] GCC is defined as the combined thickness of the RNFL, ganglion cell layer (GCL), and inner plexiform layer (Fig. 1). The segmentation was performed in a masked fashion, and every effort was made to standardize the segmentation process, which was performed by one well-trained individual and visually confirmed by a second investigator as needed.

Immunoblotting

We dissected retinae 1 day after AION induction and prepared retinal lysates. We extracted total protein in 1× radioimmunoprecipitation assay buffer (Abcam, Burlingame, CA, USA). For Western blot analysis, equal amount of protein (25 to 50 μg) was resolved by 12% Criterion XT Bis-Tris protein gel electrophoresis and transferred to polyvinylidene difluoride membranes (all from Bio-Rad, Hercules, CA, USA). Membranes were blocked with Odyssey Blocking Buffer (LI-COR, Lincoln, NE, USA) and incubated with primary antibodies against CHOP (mouse, 1:1000, Thermo Fisher Scientific, Waltham, MA, USA), control protein glyceraldehyde 3-phosphate dehydrogenase (GAPDH; rabbit, 1:2000, Cell Signaling, Danvers, MA, USA) or GRP78 (mouse, 1:1000, BD Biosciences, Franklin Lakes, NJ, USA), followed by incubation with IRDye 680-conjugated goat anti-rabbit or IRDye 800-conjugated goat anti-mouse secondary antibodies (LI-COR). We visualized positive bands on immunoblots using the Odyssey Classic Imaging System and performed densitometry analysis using Image Studio software (LI-COR).

Immunohistochemistry

At different time points after AION, we killed animals to perform immunohistochemistry. Animals were killed after deep anesthesia, and we performed intracardiac perfusion using 4% paraformaldehyde in PBS. The globe and optic nerve were dissected en bloc, processed in serial sucrose gradients (10%–30%), frozen, and cut into 12- to 15-μm sections on superfrost plus microscope glass slides for immunohistochemistry and fluorescence microscopy. For immunohistochemistry, horizontal retinal and optic nerve sections on glass slides were washed three times with washing buffer (0.5% Triton X-100 in PBS) for 10 minutes, blocked with 10% normal donkey serum in washing buffer for an hour, incubated in primary antibodies overnight in 0.3% Triton X-100 in PBS, washed three times for 10 minutes each in washing buffer, incubated with secondary antibody for 2 hours, washed three times again, and mounted with 4′,6-diamidino-2-phenylindole (DAPI)-containing mounting media (Vectashield; Vector Laboratories, Burlingame, CA, USA) using Fisherbrand cover glasses (Thermo Fisher Scientific). For primary antibodies against, we used antibodies against CHOP (1:50; catalog number MA1-250; Invitrogen, Waltham, MA, USA) and GRP78 (1:200; catalog number 610978; BD Biosciences, San Jose, CA, USA), Brn3A (1:500; catalog number Sc-31984; Santa Cruz Biotechnology, Inc., Dallas, TX, USA), GFAP (1:1000; catalog number ab4674; Abcam, Cambridge, MA, USA), and Olig2 (1:200; catalog number AB9610; Millipore Sigma, Burlington, MA, USA). For secondary antibodies, we used AlexaFluor 488 donkey anti-mouse IgG (1:500; catalog number A-21202, Invitrogen, Rockford, IL, USA), AlexaFluor 568 donkey anti-goat IgG (1:500; catalog number A-11057; Invitrogen), AlexaFluor 555 goat anti-chicken (1:500; catalog number A-21437; Invitrogen), and AlexaFluor 647 donkey anti-rabbit IgG (1:500; catalog number A-31573; Invitrogen). Sections were consistently cut and processed by one investigator and immunohistochemistry was performed by another to minimize variations. We imaged the stained retinae and optic nerves with upright epifluorescence microscopy (Nikon Eclipse TE300 microscope; Nikon Corp., Tokyo, Japan) and confocal fluorescence microscopy (Zeiss inverted LSM 880 laser scanning confocal microscope with AiryScan, Carl Zeiss, Oberkochen, Germany).

Morphometric Analyses of Retinae and Optic Nerves

To perform morphometric analysis, we took standard images of the retinae and anterior optic nerve (at the beginning of myelination zone) under masked condition with epifluorescence microscope (Nikon Eclipse E800 microscope; Nikon Corp.) using 20× objective (numerical aperture 0.75). For the retina, we imaged horizontal retinal sections near the optic nerve head using standardized parameters. To standardize region of interest (ROI) of the retinae quantified, we imaged three to four images per slide using the same magnification (20×), located 1 to 2.5 mm away from the optic nerve head. For the optic nerve, we imaged horizontal optic nerve sections in the anterior optic nerve using same high-power field and standardized parameters. To standardize area of the optic nerve counted, we used the $Olig2^+$ staining to determine the beginning of myelination, and imaged one high power field, which is 200 μm from the Bruch's membrane. Each high-power field was imaged in different channels, and image from each channel was quantified under masked condition using ImageJ (http://rsbweb.nih.gov/ij/; provided in the public domain by the National Institutes of Health, Bethesda, MD, USA). For quantification, we opened each channel of each image in ImageJ, manually applied a standard ROI in the GCL. To quantify number of $CHOP^+$ or $GRP78^+$ cells in the inner retina, we outlined a specific ROI in the GCL and manually counted the number of $CHOP^+DAPI^+$ or $GRP78^+DAPI^+$ cells in the ROI under masked condition and normalized by the length of retina. To quantify the intensity of CHOP staining in this ROI, we used the Measure tool (in artificial fluorescence unit [a.f.u.]). Quantification of the optic nerve was performed in the same way as that of retinae, except using a ROI of 0.2×0.2 mm (0.04 mm^2) at the beginning of myelination. We counted the number of $CHOP^+DAPI^+$ cells or $GRP78^+DAPI^+$ cells in the ROI, the intensity of the immunofluorescence (in a.f.u.), and area. For each data point, numbers from three to four images were averaged to calculate the value for each eye, and then data for all the eyes were used to calculate mean and standard error of the mean. For all measurements, we compared the area of the ROI as measured in ImageJ to ensure that they were identical.

Treatment of Acute AION With Chemical Chaperon 4-PBA In Vivo

To assess the effect of chemical chaperon 4-PBA on AION, we performed intraperitoneal injections of 4-PBA (40 mg/kg/d; 250 μL per injection) or PBS (control) immediately after AION induction in one eye. Animals were treated daily for a total of 19 days from day 0 to day 18. To assess effect of treatment on RGC survival, we killed the animals and performed whole mount retinal preparations, which were immunostained with antibody against Brn3A (to visualize RGCs) and then counterstained and mounted with DAPI- (to visualize nuclei) containing mounting media. We imaged the retinal and optic nerve sections using Nikon epifluorescence microscope. For quantification of retinal GCL, we took four images at 1 mm away from the optic nerve head and four images at 2.5 mm away from the optic nerve head (total two images per quadrant, eight images per eye) under masked condition (four quadrants, two images of 0.14 mm^2 each, using the 20× objective, numerical aperture, 0.75). Then, we performed morphometric analyses using a custom-written ImageJ script (ImageJ Macro, National Institutes of Health), which automatically calculates the number of $Brn3A^+$ cells per image and density of $Brn3A^+$ cells/mm^2 of retina. Each automatically performed cell count was visually reviewed under masked condition for quality control. To measure the number of optic nerve oligodendrocytes, we stained optic nerve sections (12–15 μm) with antibody against Olig2, (1:200; catalog number AB9610; Millipore Sigma), mounted in DAPI-containing mounting media (Vectashield; Vector Laboratories) and performed fluorescence microscopy (Nikon Eclipse E800 microscope; Nikon Corp.) using 20× objective. The number of $Olig2^+DAPI^+$ cells was manually counted by one investigator under masked conditions.

Statistical Analysis

To determine statistical significance for OCT and the immunohistochemistry studies, we used the Mann-Whitney *U* test. For Western blot, statistical comparisons between more than two experimental groups were made with 1-way ANOVA tests followed by Tukey multiple comparison test. Correlation was performed using Pearson correlation coefficient. All data are presented as mean ± SEM unless otherwise indicated. We performed statistical analysis using commercial statistical software Prism (GraphPad, Inc., La Jolla, CA, USA) and Microsoft Office Excel (Richmond, WA, USA). Statistical significance was defined as $P < 0.05$.

Results

Photochemical Thrombosis Model of AION and Significant Retinal Swelling 1 Day After AION

We performed photochemical thrombosis AION model in adult C57BL/6 mice.[9,71,72] Immediately after AION induction, there was expected whitening of the optic nerve head and narrowing of the peripapillary vessels (Fig. 1A). One day after AION induction, OCT imaging revealed significant thickening (swelling) of the optic nerve head in the AION eyes (Fig. 1B). The thickness of the GCC (combined RNFL, GCL, and inner plexiform layer) increased significantly by 15 μm in the AION eyes compared with contralateral, control eyes (day 0 control: 80.3 ± 0.6 μm, $n = 6$ eyes; day 0 AION: 79.2 ± 0.7 μm, $n = 6$ eyes; day 1 control: 81.3 ± 0.8 μm, $n = 6$ eyes; day 1 AION: 95 ± 2.6 μm, $n = 6$ eyes; $P < 0.0001$ 1-way ANOVA with Tukey multiple comparison test; Fig. 1C). These findings were consistent with what we reported in the past for experimental AION.[9,72]

Significant Increase in Proapoptotic ER Stress Marker CHOP and Decrease in Prosurvival ER Stress Marker GRP78 in the Retina 1 Day After AION

Given the importance of the UPR pathway in animal models of optic neuropathies and its likely importance in AION, we assessed the protein expression of the proapoptotic transcriptional factor CHOP and master chaperon GRP78 using Western blot of retinal lysates. We quantified the expression of CHOP and GRP78 as well as housekeeping molecule GAPDH[75] and compared the ratios of CHOP/GAPDH and GRP78/GAPDH in naïve, control, and day 1 AION eyes. We found that 1 day after AION, there was a significant, 10-fold increase in CHOP expression compared with naïve and control eyes (naïve: 0.0133 ± 0.0097; control: 0.0101 ± 0.0013; AION: 0.1464 ± 0.0438; $P = 0.015$, 1-way ANOVA with Tukey multiple comparison test; Fig. 2A). In contrast, there was no significant change in the GRP78/GAPDH expression 1 day after AION, although GRP78 expression decreased slightly (naïve: 1.3115 ± 0.8211; control: 0.8900 ± 0.4611; AION: 0.6126 ± 0.2709; $P = 0.65$, 1-way ANOVA with Tukey multiple comparison test; Fig. 2B).

To assess RGC-specific change in CHOP expression, we examined frozen horizontal retinal sections using immunohistochemistry and morphometric analyses. One day after AION, CHOP expression was increased in $Brn3A^+$ RGCs (Fig. 3A) and $GFAP^+$ astrocytes in the inner retina (data not shown) compared with controls. Quantification and comparison of CHOP expression in the GCL revealed that there was little $CHOP^+$ expression in control eyes, which was previously described,[43,48] and there was a significant, 6-fold increase in the number of $CHOP^+DAPI^+$ cells 1 day after AION (control: 4.9 ± 0.2 cells/mm, $n = 4$ eyes, AION: 29.6 ± 1.1 cells/mm, $n = 4$ eyes; $P = 0.03$; Mann-Whitney *U* test; Figs. 3B, 3C). There was also a significant, 3-fold increase in the intensity of CHOP expression in the GCL in AION eyes compared with controls (control: 0.57 ± 0.02 × 10^3 a.f.u., $n = 4$ eyes; AION: 1.69 ± 0.62 × 10^3 a.f.u., $n = 4$ eyes; $P = 0.03$, Mann-Whitney *U* test; Fig. 3D). Such significant increase in CHOP expression is consistent with an early and prominent increase in ER stress in retinal neurons after AION.

In contrast to CHOP, the expression of GRP78 was high in $Brn3A^+$ cells in control eyes, which was previously described,[76] and this decreased 1 day after AION (Fig. 4A). Quantification of GRP78 expression in the GCL revealed that, 1 day after AION, there was no change in the number of $GRP78^+DAPI^+$ cells in the GCL (control: 30.0 ± 1.5 cells/mm, $n = 4$ eyes; AION: 29.3 ± 1.2 cell/mm, $n = 4$ eyes; $P = 0.68$, Mann-Whitney *U* test; Figs. 4B, 4C), but there was a significant decrease in the intensity of $GRP78^+$ immunostaining in the GCL compared with controls (control: 1.44 ± 0.04 × 10^9 a.f.u., $n = 4$ eyes; AION: 0.81 ± 0.04 × 10^9 a.f.u., $n = 4$ eyes, $P = 0.03$, Mann-Whitney *U* test, Fig. 4D). Differential expression of molecules important in ER stress with an increase in the proapoptotic molecule CHOP (previous paragraph) and a decrease in the prosurvival molecule GRP78 in the retina within 1 day after AION may have additive effects that promote cell death.

Significant Increase in CHOP but No Change in GRP78 Expression in the Optic Nerve 1 Day After AION

Given AION starts in the optic nerve, we measured CHOP and GRP78 expression in the anterior optic nerve. In naïve eyes (not shown) and in contralateral control eyes on day 1, there was minimal CHOP expression in the anterior, myelinated

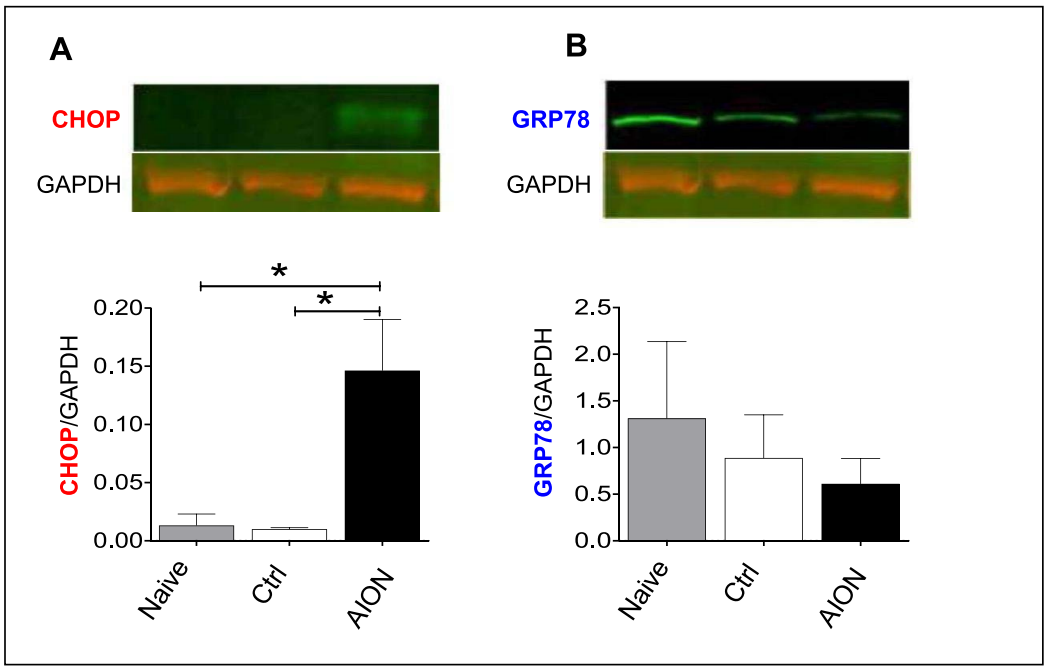

Figure 2. One day after AION, there was a 10-fold increase in CHOP protein expression (**A**) but no change in GRP78 expression (**B**) compared with naïve and contralateral, control (ctrl) eyes on Western blot. We normalized CHOP and GRP78 expression with housekeeping protein GAPDH. *P = 0.01. CHOP, CCAAT/enhancer-binding protein homologous protein; GAPDH, glyceraldehyde 3-phosphate dehydrogenase; GRP78, glucose-regulated protein 78.

portion of the optic nerve, which contains both oligodendrocytes and astrocytes (Fig. 5). One day after AION, there was high CHOP expression in the anterior optic nerve, and double labeling of CHOP$^+$Olig2$^+$ cells revealed that this increase in CHOP occurred in part in Olig2$^+$ oligodendrocytes (Fig. 5A). Quantification of CHOP$^+$DAPI$^+$ cells in the anterior optic nerve revealed a significant increase in the percentage of Olig2+ cells that are CHOP+ (control: 18.5 ± 3.6%, $n = 4$ nerves; AION: 86.8 ± 5.1%,, $n = 4$ nerves; $P = 0.03$, Mann-Whitney U test; Fig. 5C) and intensity of CHOP$^+$DAPI$^+$ cells in the optic nerve of AION eyes compared with controls 1 day after AION (control: 0.20 ± 0.01 × 10^3 a.f.u., $n = 4$ nerves; AION: 0.82 ± 0.03 ×

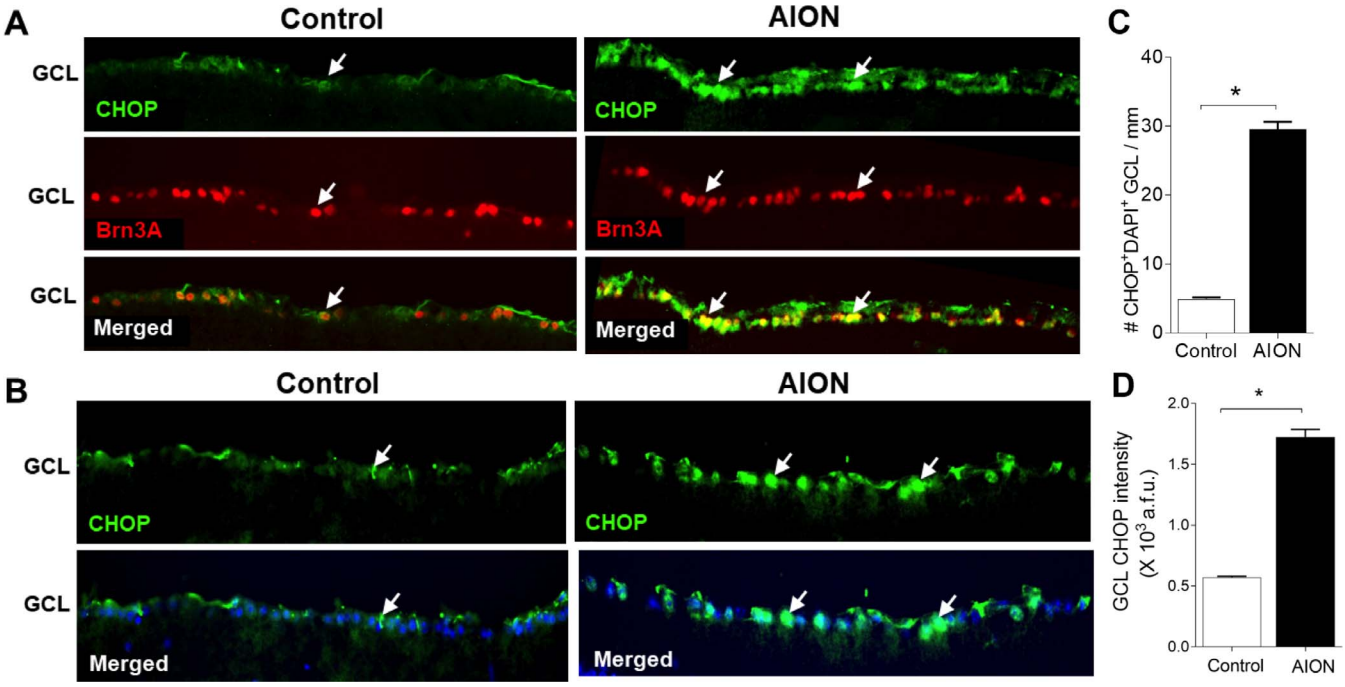

Figure 3. Significant increase of CHOP expression in the GCL 1 day after AION. (**A**) Increased CHOP$^+$Brn3A$^+$ cells in the GCL 1 day after AION. (**B**) Representative images showing increase in the number of CHOP$^+$ cells in the GCL and increase in CHOP immunoreactivity. (**C**) Bar graph showing 10-fold significant increase in CHOP$^+$DAPI$^+$ cells in the GCL 1 day after AION (*$P = 0.03$, Mann-Whitney U test). (**D**) Significant increase in the intensity of CHOP immunoreactivity in the GCL 1 day after AION (*$P = 0.03$, Mann-Whitney U test). *Scale bar*: 25 µm. GCL, ganglion cell layer.

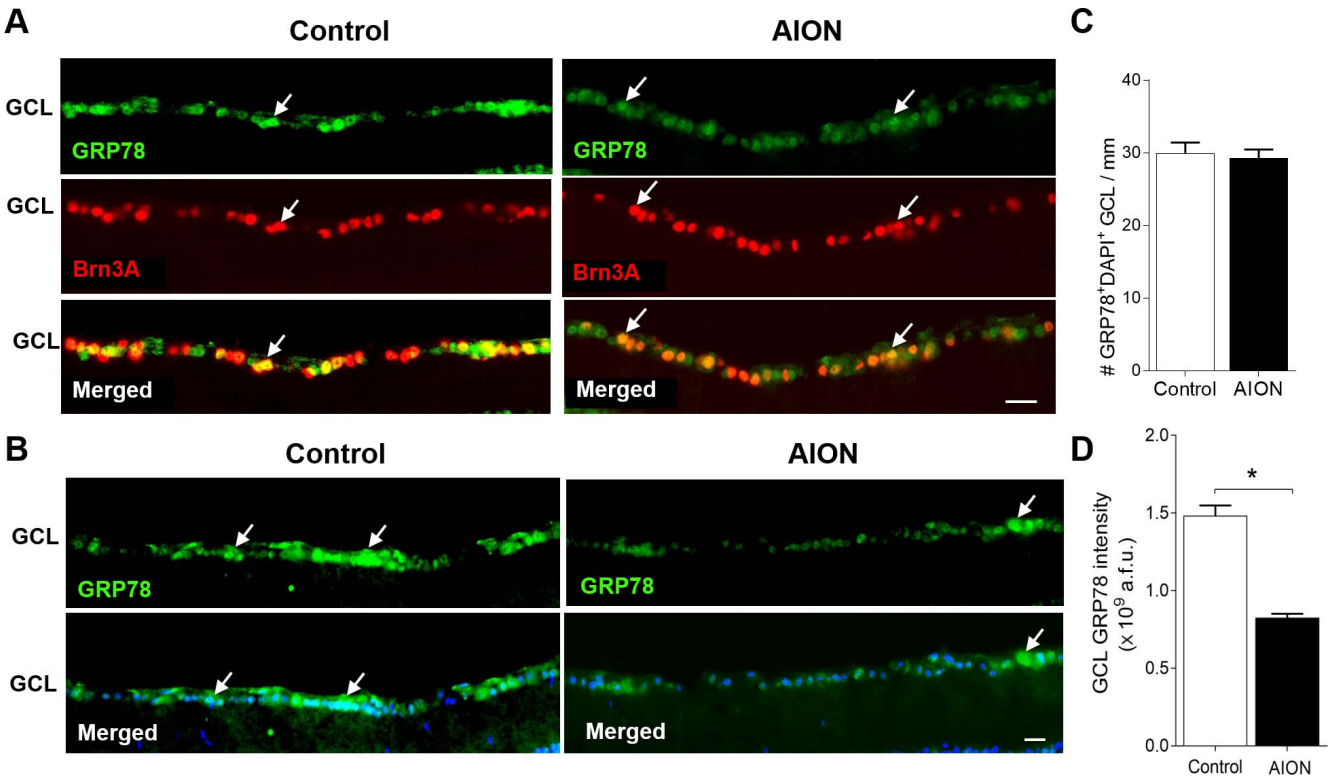

Figure 4. Significant decrease of GRP78 immunoreactivity 1 day after AION. (**A**) Reduced GRP78$^+$ immunoreactivity in Brn3A$^+$ cells in the GCL 1 day after AION. (**B**) Representative images showing relative reduction of GRP78$^+$ immunoreactivity in the GCL 1 day after AION. DAPI labels nuclei. (**C**) Bar graph showing no change in the number of GRP78$^+$DAPI$^+$ cells in the GCL. (**D**) Bar graph showing significant reduction of GRP78 immunoreactivity in the GCL 1 day after AION compared with control eyes ($n = 4$–5, $^*P = 0.03$, Mann-Whitney U test). *Scale bar*: 25 µm.

10^3 a.f.u., $n = 4$ nerves, $P = 0.03$, Mann-Whitney U test, Fig. 5D).

In contrast to CHOP, GRP78 expression in anterior optic nerve was high in naïve (not shown) and contralateral control eyes on day 1, including in Olig2$^+$ oligodendrocytes (Fig. 6A). One day after AION, there was still high GRP78 expression in the anterior optic nerve (Fig. 6A). Quantification of GRP78 label in the anterior optic nerve revealed that there was no change in the number (control: 1792.0 ± 50.7 cells/mm^2, $n =$ 3 nerves; AION: 1892.0 ± 150.2 cells/mm^2, $n = 3$ nerves, $P =$ 0.700, Mann-Whitney U test; Fig. 6C) or the intensity of GRP78 in DAPI$^+$ cells in the AION group compared with controls (control: 1.08 ± 0.17 × 10^3 a.f.u., $n = 3$ nerves; AION: 1.02 ± 0.12 × 10^3 a.f.u., $n = 3$ nerves, $P = 0.773$, Mann-Whitney U test; Fig. 6D). These findings indicated that AION was associated with differential change in molecules important in ER stress not only in the retina but also in the optic nerve glia.

Treatment With Chemical Chaperon 4-PBA Led to Significant Rescue of Brn3A$^+$ RGCs and Preserved Retinal Thickness After AION

To determine whether treatment with chemical chaperon 4-PBA, which has been shown to reduce ER stress in vitro and in vivo,[57–64] impact outcome after AION, we treated animals within 30 minutes of experimental AION (one eye AION, one eye control). The animals were treated daily for a total of 19 days of 40 mg/kg/d 4-PBA or equal volume PBS via intraperitoneal injection. We performed OCT measurements at baseline, day 1, and day 19 and killed animals at day 19 for whole mount retinal preparation and optic nerve histologic analyses (Fig. 7).

In the PBS-treated group, there was a significant 30% loss of Brn3A$^+$ RGCs in the AION eyes (loss of 700 ± 50 Brn3A$^+$ cells/mm^2) compared with the control eyes (PBS-treated control eyes: 2100 ± 61 cells/mm^2, $n = 5$; PBS-treated AION eyes: 1425 ± 154 cells/mm^2, $n = 5$ eyes, $P = 0.004$, 1-way ANOVA with Tukey multiple comparison test; Fig. 7B). With 4-PBA treatment, there was a significant, 22% rescue of RGC in the AION eyes compared with the PBS-treated AION eyes (PBS-treated AION eyes: 1425 ± 154 Brn3A$^+$ cells/mm^2, $n = 5$ eyes; 4-PBA-treated AION eyes: 1823 ± 80 Brn3A$^+$ cells/mm^2, $n = 10$ eyes; increase in 4-PBA-treated eyes by 398 ± 159 Brn3A$^+$ cells/mm^2; $P = 0.0252$, 1-way ANOVA with Tukey multiple comparison test; Figs. 7A, 7B). This meant that after 4-PBA treatment, there was no significant difference in number of Brn3A$^+$ cells in the AION eyes compared with control eyes (4-PBA-treated control eyes: 1980 ± 49 cells/mm^2, $n = 5$; 4-PBA-treated AION eyes: 1823 ± 80 cells/mm^2, $n = 10$ eyes; $P =$ 0.0777, 1-way ANOVA with Tukey multiple comparison test; Fig. 7B), which strongly supported the therapeutic efficacy of ER stress reduction in experimental AION.

Consistent with saving Brn3A$^+$ RGCs, 4-PBA-treatment also significantly preserved the GCC thickness on OCT imaging in the AION eyes. On day 19, there was a 5-µm improved thickness of the GCC in the 4-PBA-treated AION eyes compared with the PBS-treated AION eyes (day 19 PBS-treated AION eyes: 73.0 ± 1.1 µm, $n = 5$ eyes; day 19 4-PBA-treated AION eyes: 77.9 ± 1.2 µm, $n = 9$ eyes; $P = 0.01$, 1-way ANOVA with Tukey multiple comparison test; Figs. 8B, 8C). Compared with baseline at day 0, the 4-PBA-treated AION eyes at day 19 had no significant thinning of GCC (day 0 4-PBA eyes at baseline: 79.9 ± 0.5 µm, $n = 9$ eyes; day 19 4-PBA-treated AION eyes: 77.9 ± 1.2 µm, $n = 9$ eyes, $P = 0.14$, 1-way ANOVA with Tukey multiple comparison test; Figs. 8B, 8C). In

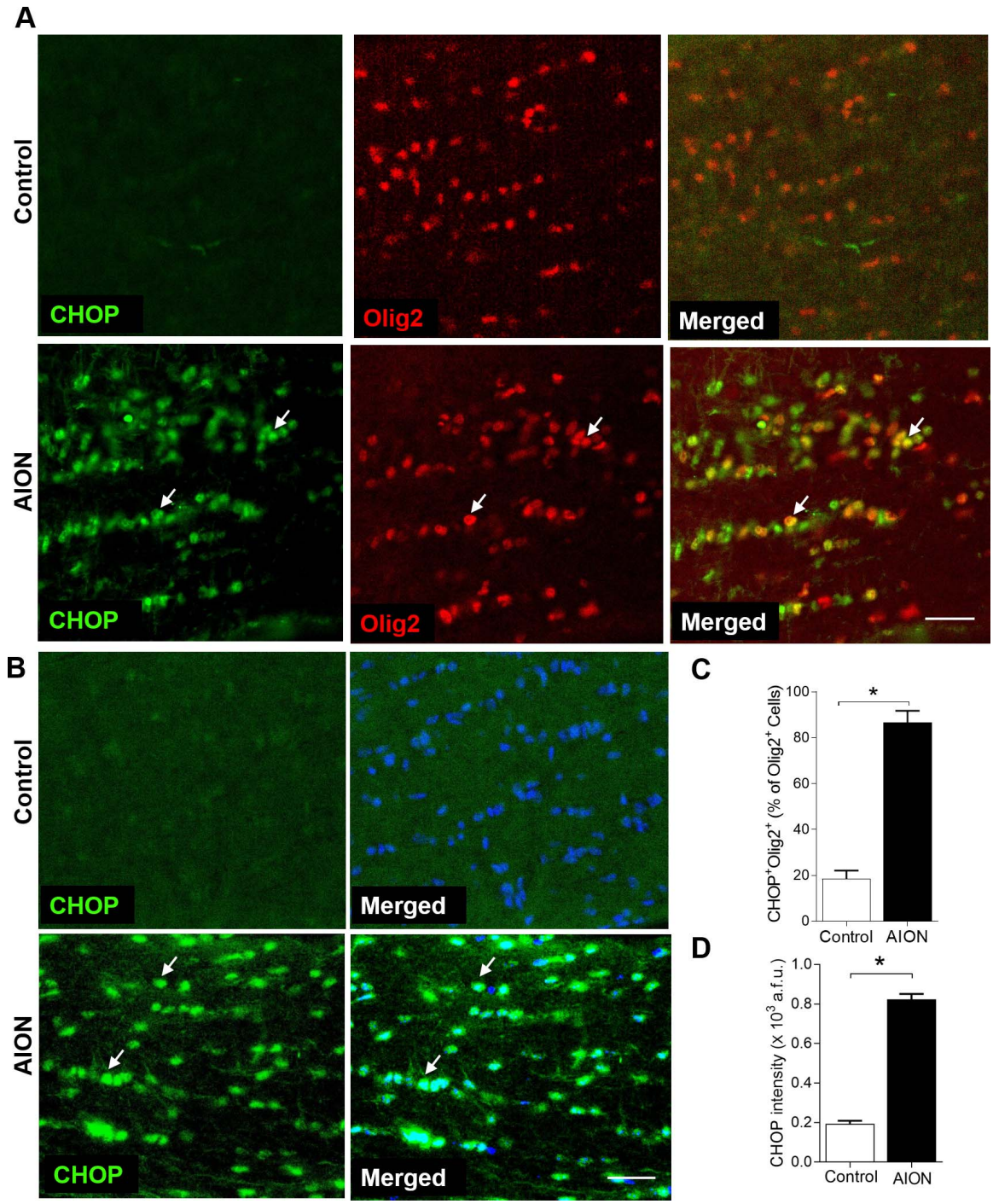

Figure 5. Significant increase of the percentage of $CHOP^+Olig2^+$ cells and intensity of CHOP immunoreactivity in the anterior optic nerve 1 day after AION. (**A**) Increase in $CHOP^+Olig2^+$ oligodendrocytes in the optic nerve 1 day after AION. (**B**) Representative images and (**C**) bar graph showing significantly increased number of $CHOP^+DAPI^+$ cells in the optic nerve 1 day after AION (*$P = 0.03$, Mann-Whitney U test). (**D**) Bar graph showing significantly increased CHOP immunoreactivity in the optic nerve 1 day after AION (*$P = 0.03$, Mann-Whitney U test). *Scale bar*: 25 µm.

contrast, in the PBS-treated AION eyes, there was 7 µm of GCC thinning compared with the same eyes at baseline (day 0 PBS-treated controls: 80 ± 0.31 µm, $n = 5$ eyes; day 19 PBS-treated AION eyes: 73.0 ± 1.1 µm, $n = 5$ eyes, $P = 0.007$, 1-way ANOVA with Tukey multiple comparison test; Fig. 8C). There was significant correlation of the $Brn3A^+$ RGC count and GCC thickness at day 19 after AION ($r = 0.5717$, $n = 10$ eyes, $P = 0.002$; Fig. 8D).

Chemical Chaperon 4-PBA Also Rescued Optic Nerve $Olig2^+$ Oligodendrocytes After AION

To assess the effect of 4-PBA treatment on oligodendrocytes after AION, we quantified the number of $Olig2^+$ optic nerve oligodendrocytes using immunohistochemical staining of frozen 15 µm horizontal sections near the optic nerve head. We found that treatment with 4-PBA led to significant preservation of

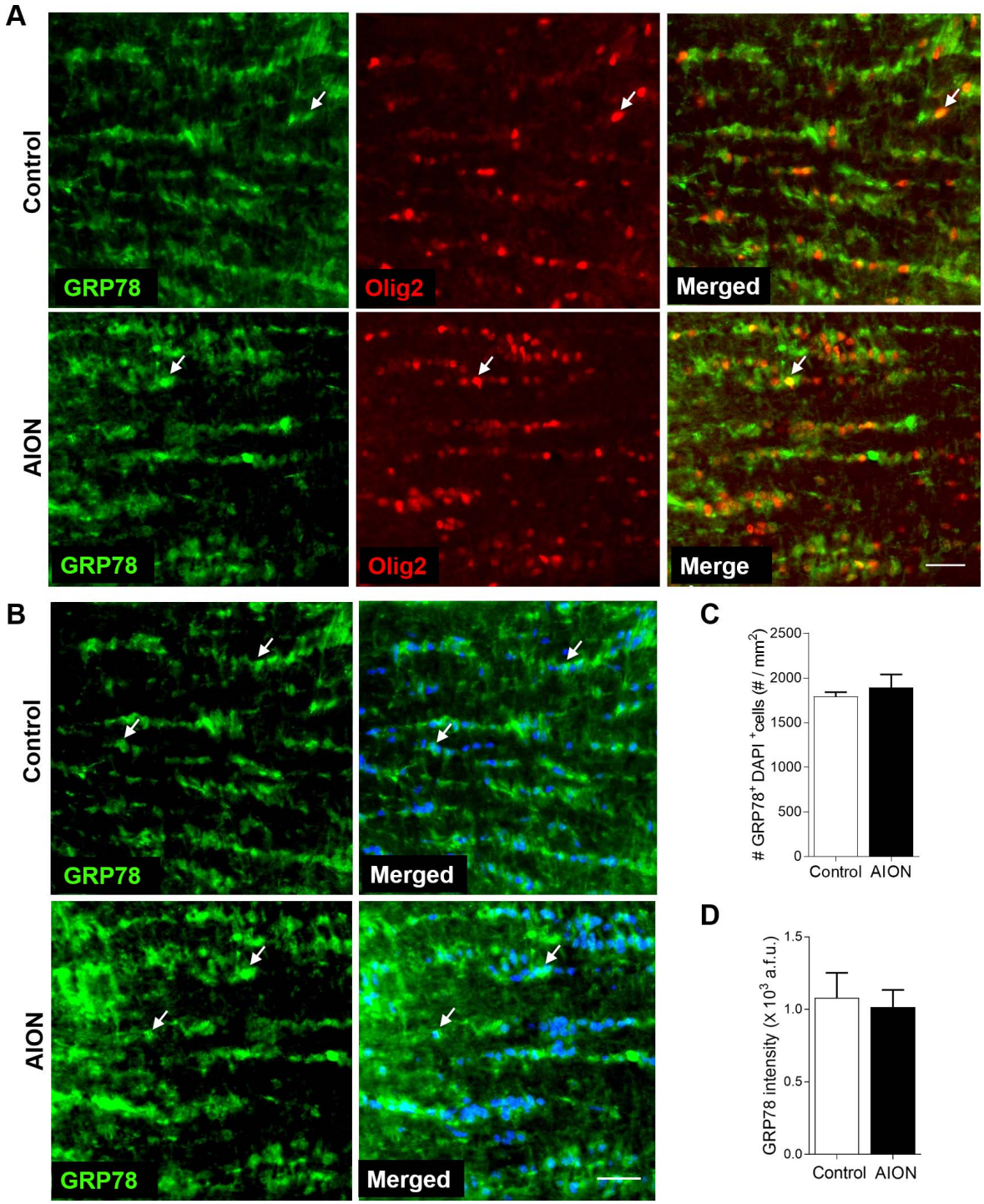

Figure 6. No change in GRP78 in the anterior optic nerve cells 1 day after AION. (**A**) No change in $GRP78^{+}Olig2^{+}$ cells in the anterior optic nerve 1 day after AION. (**B**) Representative images and (**C**) bar graph showing no change in $CHOP^{+}DAPI^{+}$ cells in the optic nerve 1 day after AION. (**D**) Bar graph showing no change in the intensity of GRP78 immunoreactivity in the anterior optic nerve 1 day after AION ($n = 4$–5, $P = 0.773$, Mann-Whitney U test). *Scale bar*: 25 μm.

$Olig2^{+}$ optic nerve oligodendrocytes 19 days after AION compared with PBS-treated AION eyes (PBS-treated AION eyes: 313 ± 39 cells/mm^2, $n = 5$; 4-PBA-treated AION eyes: 808 ± 20 cells/mm^2, $n = 5$ eyes; gain of 495 cells/mm^2; $P = 0.007$, 1-way ANOVA with Tukey multiple comparisons test; Figs. 7C, 7D). There was no change in the optic nerve cells for the non-AION control eyes under PBS and 4-PBA conditions (day 19 PBS-treated control eyes: 1044 ± 83 cells/mm^2, $n = 4$; day 19 4-PBA-treated control eyes: 1103 ± 73 cells/mm^2, $n = 5$ eyes; Fig. 7D). Despite treatment with 4-PBA, AION still resulted in loss of 27% of $Olig2^{+}$ oligodendrocytes compared with control optic nerves (4-PBA control eyes: 1103 ± 73 cells/mm^2, $n = 5$ eyes; 4-PBA AION eyes: 808 ± 20 cells/mm^2, $n = 5$ eyes, $P = 0.016$, 1-way ANOVA with Tukey multiple comparison test; Fig. 7D). However, AION eyes treated with PBS resulted in 70% cell loss compared with non-AION PBS control eye (PBS control eyes:

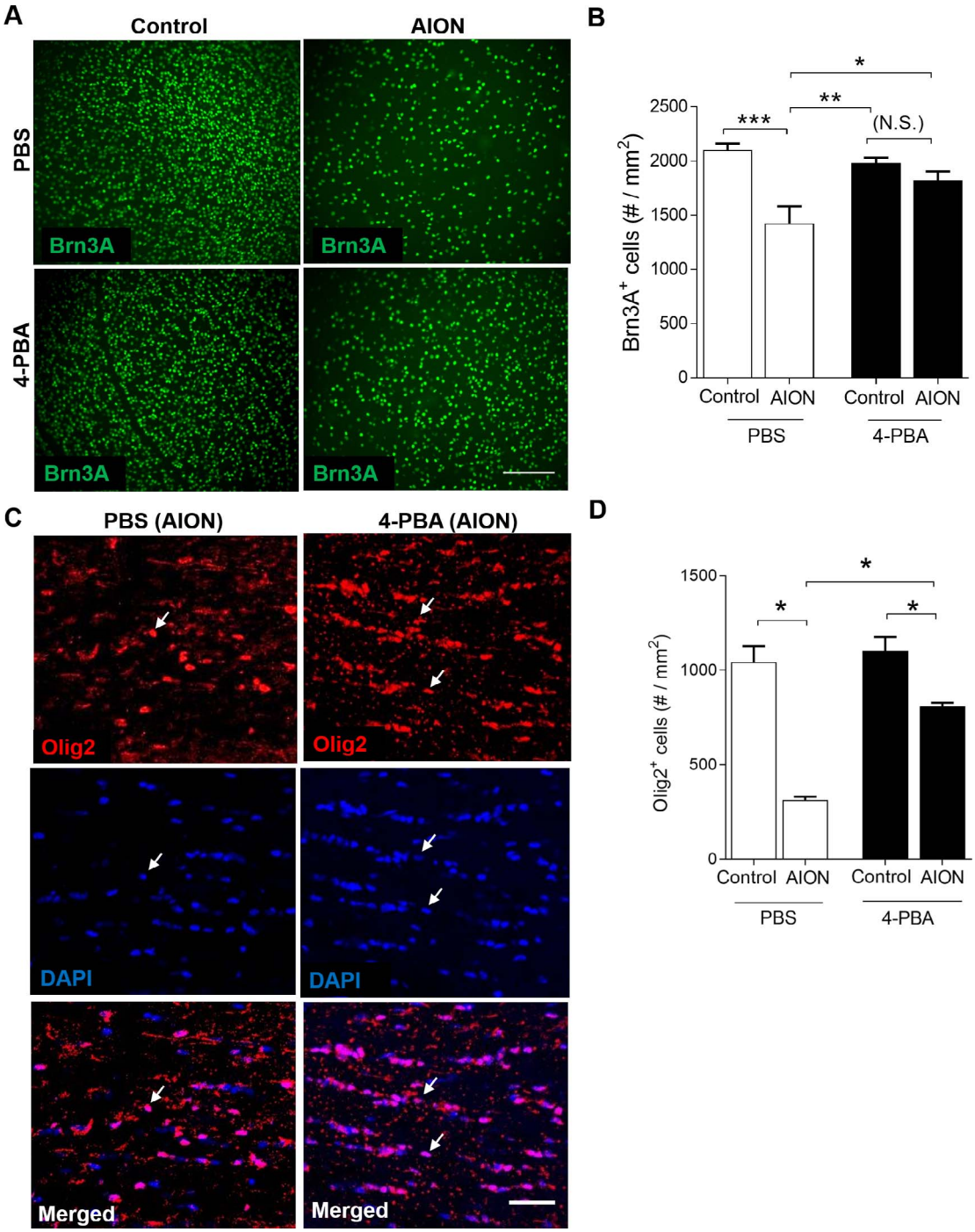

Figure 7. 4-PBA treatment for 19 days led to significant preservation of Brn3A$^+$ RGCs and Olig2$^+$ optic nerve oligodendrocytes after AION. (**A**) Representative Brn3A immunoreactivity in retinal whole mount in control (*left*) and AION (*right*) eyes after 19 days of PBS- (*top*) and 4-PBA (*bottom*) injections. *Scale bar*: 150 µm. (**B**) Bar graph showing significant preservation of Brn3A$^+$ RGCs in the 4-PBA-treated AION eyes compared with PBS-treated AION eyes ($n = 9$–10, $^*P = 0.012$, $^{**}P = 0.001$, 1-way ANOVA with Tukey multiple comparison test). There was significant loss of the Brn3A$^+$ cells in the PBS-treated AION eyes compared with controls ($^{***}P = 0.004$, 1-way ANOVA with multiple comparison test) but not in the 4-PBA-treated AION eyes compared with controls. (**C**) Representative images of Olig2$^+$DAPI$^+$ cells in the anterior optic nerve in the PBS- (*left*) and 4-PBA- (*right*) treated groups. *Scale bar*: 50 µm. (**D**) Bar graph showing significant preservation of Olig2$^+$DAPI$^+$ cells in the 4-PBA-treated AION eyes compared with PBS-treated AION eyes ($n = 5$–6, $^*P = 0.007$, 1-way ANOVA with multiple comparison test). The 4-PBA treated group had 48% more Olig2$^+$ oligodendrocytes in the anterior optic nerve compared with the PBS-treated group, although there was significant loss of Olig2$^+$ cells in both PBS- and 4-PBA-treated groups ($^*P = 0.016$ for both, 1-way ANOVA with multiple comparisons test). 4-PBA, 4-phenylbutyric acid; PBS, phosphate-buffered saline.

1044 ± 83 cells/mm^2, $n = 4$; PBS AION eyes: 313 ± 39 cells/mm^2, $n = 5$, $P = 0.016$, 1-way ANOVA with Tukey multiple comparison test; Figs. 7C, 7D). Rescue of oligodendrocytes with 4-PBA treatment also correlated with GCC thickness (RGCs: $r = 0.5717$, $n = 10$ eyes, $P = 0.002$; oligodendrocytes: $r = 0.5593$, $n = 5$ eyes, $P = 0.020$; Fig. 8E). There was no obvious difference in the pattern of optic nerve oligodendrocytes loss in the anterior or the posterior segment of the optic nerve (data not shown).

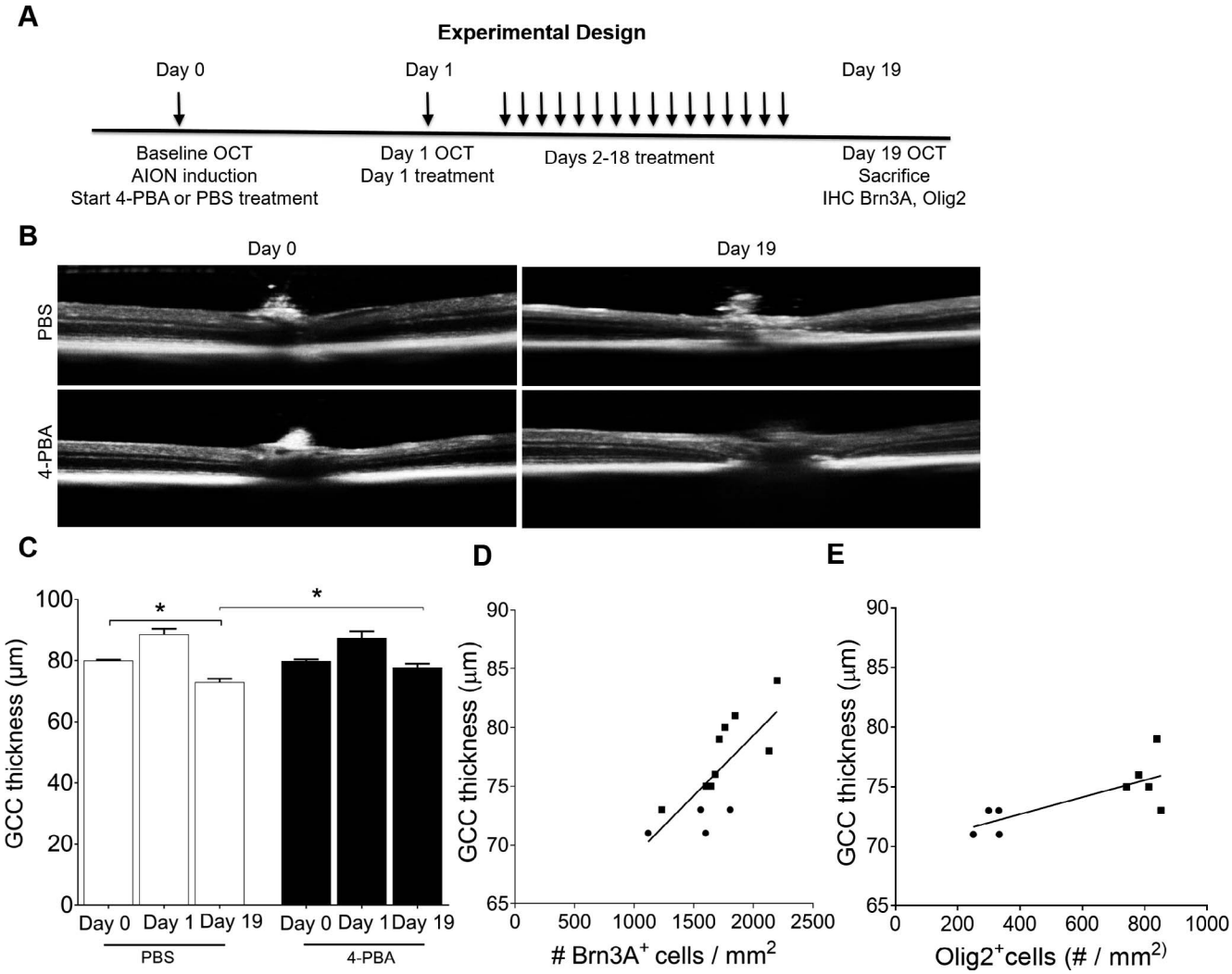

Figure 8. Treatment with 4-PBA for 19 days after AION induction significantly improved OCT GCC thickness. (**A**) Experimental design. (**B**) Representative images of OCT line scan through optic disc in PBS- (*top*) and 4-PBA- (*bottom*) treated AION eyes at day 0 (baseline) and day 19. (**C**) Bar graph showing GCC thickness in PBS- and 4-PBA-treated AION eyes on days 0, 1, and 19. There was significant thickening of GCC at day 1 in both groups and significant preservation of GCC thickness in the 4-PBA-treated AION eyes ($n = 9$–10, $^*P = 0.01$, 1-way ANOVA with Tukey multiple comparison test). Scatter plots showing correlation between GCC thickness and the number of Brn3A$^+$ cells in retina (**D**) and Olig2$^+$ cells (**E**) in the anterior optic nerve in the all the eyes after 19 days post AION (both PBS and 4-PBA-treated groups). GCC versus Brn3A$^+$ RGCs: $r = 0.5717$, $n = 10$ eyes, $P = 0.002$; GCC versus Olig2$^+$ oligodendrocytes: $r = 0.5593$, $n = 5$ eyes, $P = 0.02$ (*circle* and *square* shape represent PBS and 4-PBA treated eyes, respectively). IHC, immunohistochemistry.

Discussion

Our study revealed that 1 day after AION, there was a significant, differential expression of molecules of the UPR pathway, with increase in protein expression of the proapoptotic transcription factor CHOP and decrease in protein expression of the prosurvival master chaperon GRP78 in the retina. In the optic nerve, there was also significant change in the expression of CHOP but not GRP78. Such differential expression of UPR pathway supports a model of AION mechanism of disease where increased ER stress occurs in both RGCs and optic nerve glia shortly after insult. This then leads to rapid activation of both intrinsic (RGCs) and extrinsic (oligodendrocytes, astrocytes) mechanisms that likely impact the survival of RGC soma and axons, although we do not know whether there is interaction between the two mechanisms. Consistent with the idea that ER stress plays a role in pathogenesis of AION, treatment with chemical chaperon 4-PBA, which has been shown to reduce ER stress in vitro and in vivo,[57–64] significantly preserved both Brn3A$^+$ RGCs and Olig2$^+$ oligodendrocytes in the anterior optic nerve after AION.

Other than our study on AION, differential regulation of GRP78 and CHOP expression, that is, reduced GRP78 and increased CHOP expression, has been found in RGCs in animal models of optic neuritis and traumatic optic neuropathy.[77] Similarly, successful treatment of experimental optic neuropathies and improved RGC survival[77,78] have also been associated with differential expression of GRP78 and CHOP in the opposite direction, that is, increased GRP78[79] and decreased CHOP expression in cells in the RGC layer. Nakamura et al.[78] showed that RGC loss after optic nerve crush animal model was associated with decreased GRP78 and increased CHOP expression and that treatment with bilberry extract anthocyanins led to improved RGC survival, increased GRP78 and decreased CHOP expressions, along with reduced expression of *BAX* and *ATF4*, which are downstream of *DDIT3* (CHOP). Jiang et al.[77] showed that transplantation of human umbilical cord cells as treatment for traumatic optic neurop-

athy animal model led to improved RGC survival and increase in expression of GRP78 and decrease in expression of CHOP.

Although 4-PBA treatment after retinal ischemia (via high intraocular pressure) had no effect on survival of retinal neurons,[57] our data showed that 4-PBA treatment after AION led to improved RGC and optic nerve oligodendrocyte survival. Future studies are needed to determine whether 4-PBA treatment indeed modulates ER stress as a means of exerting these effects in AION. 4-PBA has also been shown to rescue RGCs in retinal ischemia-reperfusion injury,[57] glucocorticoid-induced ocular hypertension,[64] and Leber congenital amaurosis[80] as well as oligodendrocytes in spinal cord injury.[81] Although we showed that 4-PBA rescued retinal neurons and optic nerve oligodendrocytes after AION, we do not know whether this is a direct effect of 4-PBA on RGCs and oligodendrocytes or there may be interaction between the two (e.g., rescue of RGCs led to preservation of the optic nerve oligodendrocytes or vice versa). If chemical chaperon has independent effects on both retinal neurons and optic nerve oligodendrocytes, reduction of ER stress would be an ideal type of therapy to treat AION or other optic neuropathies, given visual restoration requires that RGCs, the axons, and the optic nerve oligodendrocytes survive and function well. The reduction of CHOP expression in the retina and optic nerve after 4-PBA provides support that 4-PBA may reduce ER stress in both cell types.

In a study of middle cerebral artery occlusion in rat, 4-PBA had a significant impact on the level of astrogliosis, and this impacted neuronal survival after stroke.[70] In models of multiple sclerosis and other CNS diseases, ER stress has been associated with neuroinflammation.[82–84] 4-PBA treatment has been shown to reduce the expression of inducible nitric-oxide synthase, TNFα, which may have a role in dampening post-ischemic inflammation.[66] In a rat stroke model, treatment within 1 hour of ischemia was better than 3 hours, although animals in both groups improved over days.[66] Higher dose of 4-PBA (120 mg/kg/d) was associated with better outcome than 15 or 40 mg/kg/d.[66]

Different studies have shown that treatment with 4-PBA can reduce ER stress and salvage neurons. Retinal CHOP was significantly increased in the inner retina after high intraocular pressure-induced ischemia.[41,43,85] In a study of high intraocular pressure-induced retinal ischemia in rats, pretreatment with 100 or 400 mg/kg rescued 100% of RGCs, while posttreatment 1 hour after ischemia with either dose had no effect on retinal neurons.[57] In a study of middle cerebral artery occlusion in rat, 4-PBA had a significant impact on the level of astrogliosis, and this might have impacted neuronal survival after stroke.[70] Most of the studies of CNS stroke have focused on neurons, and the data on this is mixed. In a mouse[66] and a rat[60] study of stroke, there was postischemic increase in GRP78, CHOP, activation of caspase-12, and number of $TUNEL^+$ (terminal deoxynucleotidyl transferase-mediated dUTP nick end labeling) cells. An in vitro and in vivo study of stroke revealed that there was decreased ER stress protein expression (eIF2α and ATF4) at 3 hours of reperfusion in CA3 hippocampal neurons following ischemia and increase in CA1 neurons at 12 hours of reperfusion.

Chemical chaperons like sodium phenylbutyrate and other drugs that act on the UPR pathway and promote cell survival are already in routine clinical use and is approved by the US Food and Drug Administration for the treatment of metabolic diseases.[86,87] The older drug sodium phenylbutyrate (Buphenyl) ($C_{10}H_{11}O_2Na$, molecular weight 180) has been used to treat urea cycle abnormality and cystic fibrosis. More recently, glycerol phenylbutyrate (a pre-pro drug converted to three molecules of phenylbutyric acid [PBA] by pancreatic lipases that was approved by the US Food and Drug Administration in 2013) is a better tolerated drug and is associated with fewer side effects.[88] Other than sodium and glycerol phenylbutyrate, there are other drugs that manipulate different aspects of the ER stress pathway and are potential therapeutic considerations for treatment of AION.[89]

Limitations of our study include photochemical thrombosis model to simulate human nonarteritic AION as discussed above. Also, we only focused on the two most important UPR molecules in acute AION, and it will be important to perform a more detailed study to investigate the temporal and spatial expression patterns of different members of the ER stress pathway at different times after AION, the effect of ER stress reduction with chemical chaperons (e.g., oral glycerol phenylbutyrate treatment after experimental AION), and the functional impact of treatment using optokinetic responses[90,91] or visual evoked potential recordings.[92]

Our study highlights the clinical relevance of ER stress in two aspects of human nonarteritic AION. First, increased ER stress may be one of the earliest biomarkers of cell death in RGCs and a measurement of ER stress in vivo, through retinal imaging, blood testing, or other ways, may be useful to monitor patients and determine their likelihood of responding to treatment that reduces ER stress. Second, treatment to reduce ER stress has not been used as treatment for loss of oxygen, including stroke, AION, and other conditions. Given our findings in animal studies that ER stress reduction can salvage retinal neurons and optic nerve oligodendrocytes, which are both critical for vision restoration, ER stress reduction is a novel therapeutic approach for this devastating human condition. It is important to emphasize that the human nonarteritic AION and photochemical thrombosis rodent model of AION are not the same, so if this drug is confirmed in future studies to be of likely benefit in the treatment of AION, a careful study of its efficacy in patients with nonarteritic AION should be done. This is most ideally done as a prospective, randomized, placebo-controlled clinical trial.

Acknowledgments

The authors thank Ming-Hui Sun, MD, PhD, and Roopa Dalal for their help in experiments.

Some of these results were presented at the 2018 North American Neuro-Ophthalmology meeting and the 2018 Association for Research in Vision and Ophthalmology meeting.

Supported by the Career Award in Biomedical Sciences from the Burroughs Wellcome Foundation, Weston Havens Foundation, the North American Neuro-Ophthalmology Society Pilot Grant, Bonderman Gift Grant, Research to Prevent Blindness, Inc., National Eye Institute P30-026877 grant (YJL), and the American Heart Association Postdoctoral Fellowship (18POST34030385) (VK).

Disclosure: **V. Kumar**, None; **L.A. Mesentier-Louro**, None; **A.J. Oh**, None; **K. Heng**, None; **M.A. Shariati**, None; **H. Huang**, None; **Y. Hu**, None; **Y.J. Liao**, None

References

1. Hayreh SS. Anterior ischaemic optic neuropathy. III. Treatment, prophylaxis, and differential diagnosis. *Br J Ophthalmol.* 1974;58:981–989.
2. Arnold AC. Pathogenesis of nonarteritic anterior ischemic optic neuropathy. *J Neuroophthalmol.* 2003;23:157–163.
3. Hayreh SS. Ischemic optic neuropathy. *Prog Retin Eye Res.* 2009;28:34–62.
4. Beri M, Klugman MR, Kohler JA, Hayreh SS. Anterior ischemic optic neuropathy. VII. Incidence of bilaterality and various influencing factors. *Ophthalmology.* 1987;94:1020–1028.

5. Knox DL, Kerrison JB, Green WR. Histopathologic studies of ischemic optic neuropathy. *Trans Am Ophthalmol Soc*. 2000; 98:203–220; discussion 221–222.
6. Bernstein SL, Guo Y, Kelman SE, Flower RW, Johnson MA. Functional and cellular responses in a novel rodent model of anterior ischemic optic neuropathy. *Invest Ophthalmol Vis Sci*. 2003;44:4153–4162.
7. Goldenberg-Cohen N, Guo Y, Margolis F, Cohen Y, Miller NR, Bernstein SL. Oligodendrocyte dysfunction after induction of experimental anterior optic nerve ischemia. *Invest Ophthalmol Vis Sci*. 2005;46:2716–2725.
8. Pangratz-Fuehrer S, Kaur K, Ousman SS, Steinman L, Liao YJ. Functional rescue of experimental ischemic optic neuropathy with alphaB-crystallin. *Eye (Lond)*. 2011;25:809–817.
9. Ho JK, Stanford M, Shariati MA, Dalal R, Liao YJ. Optical coherence tomography study of experimental anterior ischemic optic neuropathy and histologic confirmation. *Invest Ophthalmol Vis Sci*. 2013;54:5981–5988.
10. Yu C, Ho JK, Liao YJ. Subretinal fluid is common in experimental non-arteritic anterior ischemic optic neuropathy. *Eye (Lond)*. 2014;28:1494–1501.
11. Bernstein SL, Johnson MA, Miller NR. Nonarteritic anterior ischemic optic neuropathy (NAION) and its experimental models. *Prog Retin Eye Res*. 2011;30:167–187.
12. Slater BJ, Vilson FL, Guo Y, Weinreich D, Hwang S, Bernstein SL. Optic nerve inflammation and demyelination in a rodent model of nonarteritic anterior ischemic optic neuropathy. *Invest Ophthalmol Vis Sci*. 2013;54:7952–7961.
13. Chen CS, Johnson MA, Flower RA, Slater BJ, Miller NR, Bernstein SL. A primate model of nonarteritic anterior ischemic optic neuropathy. *Invest Ophthalmol Vis Sci*. 2008;49:2985–2992.
14. Salgado C, Vilson F, Miller NR, Bernstein SL. Cellular inflammation in nonarteritic anterior ischemic optic neuropathy and its primate model. *Arch Ophthalmol*. 2011;129: 1583–1591.
15. Dratviman-Storobinsky O, Hasanreisoglu M, Offen D, Barhum Y, Weinberger D, Goldenberg-Cohen N. Progressive damage along the optic nerve following induction of crush injury or rodent anterior ischemic optic neuropathy in transgenic mice. *Mol Vis*. 2008;14:2171–2179.
16. Slater BJ, Mehrabian Z, Guo Y, Hunter A, Bernstein SL. Rodent anterior ischemic optic neuropathy (rAION) induces regional retinal ganglion cell apoptosis with a unique temporal pattern. *Invest Ophthalmol Vis Sci*. 2008;49:3671–3676.
17. Zhang C, Guo Y, Slater BJ, Miller NR, Bernstein SL. Axonal degeneration, regeneration and ganglion cell death in a rodent model of anterior ischemic optic neuropathy (rAION). *Exp Eye Res*. 2010;91:286–292.
18. Shariati MA, Kumar V, Yang T, et al. A Small molecule TrkB neurotrophin receptor partial agonist as possible treatment for experimental nonarteritic anterior ischemic optic neuropathy. *Curr Eye Res*. 2018;43:1489–1499.
19. Johnson MA, Miller NR, Nolan T, Bernstein SL. Peripapillary retinal nerve fiber layer swelling predicts peripapillary atrophy in a primate model of nonarteritic anterior ischemic optic neuropathy. *Invest Ophthalmol Vis Sci*. 2016;57:527–532.
20. Ron D, Walter P. Signal integration in the endoplasmic reticulum unfolded protein response. *Nat Rev Mol Cell Biol*. 2007;8:519–529.
21. Han J, Kaufman RJ. Physiological/pathological ramifications of transcription factors in the unfolded protein response. *Genes Dev*. 2017;31:1417–1438.
22. Lee AS. The ER chaperone and signaling regulator GRP78/BiP as a monitor of endoplasmic reticulum stress. *Methods*. 2005; 35:373–381.
23. Wang M, Wey S, Zhang Y, Ye R, Lee AS. Role of the unfolded protein response regulator GRP78/BiP in development, cancer, and neurological disorders. *Antioxid Redox Signal*. 2009;11:2307–2316.
24. Wang S, Kaufman RJ. The impact of the unfolded protein response on human disease. *J Cell Biol*. 2012;197:857–867.
25. Zhang HY, Wang ZG, Lu XH, et al. Endoplasmic reticulum stress: relevance and therapeutics in central nervous system diseases. *Mol Neurobiol*. 2015;51:1343–1352.
26. Wang M, Kaufman RJ. Protein misfolding in the endoplasmic reticulum as a conduit to human disease. *Nature*. 2016;529: 326–335.
27. Zhang SX, Ma JH, Bhatta M, Fliesler SJ, Wang JJ. The unfolded protein response in retinal vascular diseases: implications and therapeutic potential beyond protein folding. *Prog Retin Eye Res*. 2015;45:111–131.
28. Kroeger H, Chiang WC, Felden J, Nguyen A, Lin JH. ER stress and unfolded protein response in ocular health and disease. *FEBS J*. 2019;286:399–412.
29. Jing G, Wang JJ, Zhang SX. ER stress and apoptosis: a new mechanism for retinal cell death. *Exp Diabetes Res*. 2012; 2012:589589.
30. Zhang SX, Sanders E, Fliesler SJ, Wang JJ. Endoplasmic reticulum stress and the unfolded protein responses in retinal degeneration. *Exp Eye Res*. 2014;125:30–40.
31. Doh SH, Kim JH, Lee KM, Park HY, Park CK. Retinal ganglion cell death induced by endoplasmic reticulum stress in a chronic glaucoma model. *Brain Res*. 2010;1308:158–166.
32. Hu Y, Park KK, Yang L, et al. Differential effects of unfolded protein response pathways on axon injury-induced death of retinal ganglion cells. *Neuron*. 2012;73:445–452.
33. Yang L, Li S, Miao L, et al. Rescue of glaucomatous neurodegeneration by differentially modulating neuronal endoplasmic reticulum stress molecules. *J Neurosci*. 2016; 36:5891–5903.
34. Li J, Wang JJ, Yu Q, Wang M, Zhang SX. Endoplasmic reticulum stress is implicated in retinal inflammation and diabetic retinopathy. *FEBS Lett*. 2009;583:1521–1527.
35. Drel VR, Xu W, Zhang J, et al. Poly(ADP-ribose)polymerase inhibition counteracts cataract formation and early retinal changes in streptozotocin-diabetic rats. *Invest Ophthalmol Vis Sci*. 2009;50:1778–1790.
36. Oshitari T, Yoshida-Hata N, Yamamoto S. Effect of neurotrophic factors on neuronal apoptosis and neurite regeneration in cultured rat retinas exposed to high glucose. *Brain Res*. 2010;1346:43–51.
37. Oshitari T, Yoshida-Hata N, Yamamoto S. Effect of neurotrophin-4 on endoplasmic reticulum stress-related neuronal apoptosis in diabetic and high glucose exposed rat retinas. *Neurosci Lett*. 2011;501:102–106.
38. Shimazawa M, Miwa A, Ito Y, Tsuruma K, Aihara M, Hara H. Involvement of endoplasmic reticulum stress in optic nerve degeneration following N-methyl-D-aspartate-induced retinal damage in mice. *J Neurosci Res*. 2012;90:1960–1969.
39. Huang H, Miao L, Liang F, et al. Neuroprotection by eIF2alpha-CHOP inhibition and XBP-1 activation in EAE/optic neuritis. *Cell Death Dis*. 2017;8:e2936.
40. Krajewska M, Xu L, Xu W, et al. Endoplasmic reticulum protein BI-1 modulates unfolded protein response signaling and protects against stroke and traumatic brain injury. *Brain Res*. 2011;1370:227–237.
41. Li C, Wang L, Huang K, Zheng L. Endoplasmic reticulum stress in retinal vascular degeneration: protective role of resveratrol. *Invest Ophthalmol Vis Sci*. 2012;53:3241–3249.
42. Hata N, Oshitari T, Yokoyama A, Mitamura Y, Yamamoto S. Increased expression of IRE1alpha and stress-related signal

Investigative Ophthalmology & Visual Science

transduction proteins in ischemia-reperfusion injured retina. *Clin Ophthalmol*. 2008;2:743–752.

43. Nashine S, Liu Y, Kim BJ, Clark AF, Pang IH. Role of C/EBP homologous protein in retinal ganglion cell death after ischemia/reperfusion injury. *Invest Ophthalmol Vis Sci*. 2014;56:221–231.
44. Lin JH, Li H, Yasumura D, et al. IRE1 signaling affects cell fate during the unfolded protein response. *Science*. 2007;318: 944–949.
45. Yasuda M, Tanaka Y, Ryu M, Tsuda S, Nakazawa T. RNA sequence reveals mouse retinal transcriptome changes early after axonal injury. *PLoS One*. 2014;9:e93258.
46. Baltan S. Age-specific localization of NMDA receptors on oligodendrocytes dictates axon function recovery after ischemia. *Neuropharmacology*. 2016;110:626–632.
47. Rathnasamy G, Murugan M, Ling EA, Kaur C. Hypoxia-induced iron accumulation in oligodendrocytes mediates apoptosis by eliciting endoplasmic reticulum stress. *Mol Neurobiol*. 2016; 53:4713–4727.
48. Ojino K, Shimazawa M, Izawa H, Nakano Y, Tsuruma K, Hara H. Involvement of endoplasmic reticulum stress in optic nerve degeneration after chronic high intraocular pressure in DBA/2J mice. *J Neurosci Res*. 2015;93:1675–1683.
49. Benavides A, Pastor D, Santos P, Tranque P, Calvo S. CHOP plays a pivotal role in the astrocyte death induced by oxygen and glucose deprivation. *Glia*. 2005;52:261–275.
50. Lewis GP, Fisher SK. Up-regulation of glial fibrillary acidic protein in response to retinal injury: its potential role in glial remodeling and a comparison to vimentin expression. *Int Rev Cytol*. 2003;230:263–290.
51. Ma T, Trinh MA, Wexler AJ, et al. Suppression of eIF2alpha kinases alleviates Alzheimer's disease-related plasticity and memory deficits. *Nat Neurosci*. 2013;16:1299–1305.
52. Valdes P, Mercado G, Vidal RL, et al. Control of dopaminergic neuron survival by the unfolded protein response transcription factor XBP1. *Proc Natl Acad Sci U S A*. 2014;111:6804–6809.
53. Kim HJ, Raphael AR, LaDow ES, et al. Therapeutic modulation of eIF2alpha phosphorylation rescues TDP-43 toxicity in amyotrophic lateral sclerosis disease models. *Nat Genet*. 2014;46:152–160.
54. Saxena S, Cabuy E, Caroni P. A role for motoneuron subtype-selective ER stress in disease manifestations of FALS mice. *Nat Neurosci*. 2009;12:627–636.
55. Valenzuela V, Collyer E, Armentano D, Parsons GB, Court FA, Hetz C. Activation of the unfolded protein response enhances motor recovery after spinal cord injury. *Cell Death Dis*. 2012; 3:e272.
56. McMahon JM, McQuaid S, Reynolds R, FitzGerald UF. Increased expression of ER stress- and hypoxia-associated molecules in grey matter lesions in multiple sclerosis. *Mult Scler*. 2012;18:1437–1447.
57. Jeng YY, Lin NT, Chang PH, et al. Retinal ischemic injury rescued by sodium 4-phenylbutyrate in a rat model. *Exp Eye Res*. 2007;84:486–492.
58. Jian L, Lu Y, Lu S, Lu C. Chemical chaperone 4-phenylbutyric acid protects H9c2 cardiomyocytes from ischemia/reperfusion injury by attenuating endoplasmic reticulum stress-induced apoptosis. *Mol Med Rep*. 2016;13:4386–4392.
59. Mizukami T, Orihashi K, Herlambang B, et al. Sodium 4-phenylbutyrate protects against spinal cord ischemia by inhibition of endoplasmic reticulum stress. *J Vasc Surg*. 2010;52:1580–1586.
60. Srinivasan K, Sharma SS. Sodium phenylbutyrate ameliorates focal cerebral ischemic/reperfusion injury associated with comorbid type 2 diabetes by reducing endoplasmic reticulum stress and DNA fragmentation. *Behav Brain Res*. 2011;225: 110–116.
61. Tung WF, Chen WJ, Hung HC, et al. 4-Phenylbutyric acid (4-PBA) and lithium cooperatively attenuate cell death during oxygen-glucose deprivation (OGD) and reoxygenation. *Cell Mol Neurobiol*. 2015;35:849–859.
62. Zode GS, Bugge KE, Mohan K, et al. Topical ocular sodium 4-phenylbutyrate rescues glaucoma in a myocilin mouse model of primary open-angle glaucoma. *Invest Ophthalmol Vis Sci*. 2012;53:1557–1565.
63. Zode GS, Kuehn MH, Nishimura DY, et al. Reduction of ER stress via a chemical chaperone prevents disease phenotypes in a mouse model of primary open angle glaucoma. *J Clin Invest*. 2011;121:3542–3553.
64. Zode GS, Sharma AB, Lin X, et al. Ocular-specific ER stress reduction rescues glaucoma in murine glucocorticoid-induced glaucoma. *J Clin Invest*. 2014;124:1956–1965.
65. Dasgupta S, Zhou Y, Jana M, Banik NL, Pahan K. Sodium phenylacetate inhibits adoptive transfer of experimental allergic encephalomyelitis in SJL/J mice at multiple steps. *J Immunol*. 2003;170:3874–3882.
66. Qi X, Hosoi T, Okuma Y, Kaneko M, Nomura Y. Sodium 4-phenylbutyrate protects against cerebral ischemic injury. *Mol Pharmacol*. 2004;66:899–908.
67. Grall S, Prunier-Mirebeau D, Tamareille S, et al. Endoplasmic reticulum stress pathway involvement in local and remote myocardial ischemic conditioning. *Shock*. 2013;39:433–439.
68. Zhang C, Tang Y, Li Y, et al. Unfolded protein response plays a critical role in heart damage after myocardial ischemia/reperfusion in rats. *PLoS One*. 2017;12:e0179042.
69. Takatori O, Usui S, Okajima M, et al. Sodium 4-phenylbutyrate attenuates myocardial reperfusion injury by reducing the unfolded protein response. *J Cardiovasc Pharmacol Ther*. 2017;22:283–292.
70. Yoshikawa A, Kamide T, Hashida K, et al. Deletion of Atf6alpha impairs astroglial activation and enhances neuronal death following brain ischemia in mice. *J Neurochem*. 2015; 132:342–353.
71. Yu C, Ho JK, Liao YJ. Subretinal fluid is common in experimental non-arteritic anterior ischemic optic neuropathy. *Eye (Lond)*. 2014;28:1494–1501.
72. Shariati MA, Park JH, Liao YJ. Optical coherence tomography study of retinal changes in normal aging and after ischemia. *Invest Ophthalmol Vis Sci*. 2015;56:2790–2797.
73. Nakano N, Ikeda HO, Hangai M, et al. Longitudinal and simultaneous imaging of retinal ganglion cells and inner retinal layers in a mouse model of glaucoma induced by N-methyl-D-aspartate. *Invest Ophthalmol Vis Sci*. 2011;52: 8754–8762.
74. Hein K, Gadjanski I, Kretzschmar B, et al. An optical coherence tomography study on degeneration of retinal nerve fiber layer in rats with autoimmune optic neuritis. *Invest Ophthalmol Vis Sci*. 2012;53:157–163.
75. Barber RD, Harmer DW, Coleman RA, Clark BJ. GAPDH as a housekeeping gene: analysis of GAPDH mRNA expression in a panel of 72 human tissues. *Physiol Genomics*. 2005;21:389–395.
76. Quinones QJ, de Ridder GG, Pizzo SV. GRP78: a chaperone with diverse roles beyond the endoplasmic reticulum. *Histol Histopathol*. 2008;23:1409–1416.
77. Jiang B, Zhang P, Zhou D, Zhang J, Xu X, Tang L. Intravitreal transplantation of human umbilical cord blood stem cells protects rats from traumatic optic neuropathy. *PLoS One*. 2013;8:e69938.
78. Nakamura O, Moritoh S, Sato K, et al. Bilberry extract administration prevents retinal ganglion cell death in mice via the regulation of chaperone molecules under conditions of endoplasmic reticulum stress. *Clin Ophthalmol*. 2017;11: 1825–1834.

Investigative Ophthalmology & Visual Science

79. Goldenberg-Cohen N, Raiter A, Gaydar V, et al. Peptide-binding GRP78 protects neurons from hypoxia-induced apoptosis. *Apoptosis*. 2012;17:278–288.
80. Li S, Samardzija M, Yang Z, Grimm C, Jin M. Pharmacological amelioration of cone survival and vision in a mouse model for Leber congenital amaurosis. *J Neurosci*. 2016;36:5808–5819.
81. Zhou Y, Ye L, Zheng B, et al. Phenylbutyrate prevents disruption of blood-spinal cord barrier by inhibiting endoplasmic reticulum stress after spinal cord injury. *Am J Transl Res*. 2016;8:1864–1875.
82. Sprenkle NT, Sims SG, Sanchez CL, Meares GP. Endoplasmic reticulum stress and inflammation in the central nervous system. *Mol Neurodegener*. 2017;12:42.
83. Wang Z, Huang Y, Cheng Y, et al. Endoplasmic reticulum stress-induced neuronal inflammatory response and apoptosis likely plays a key role in the development of diabetic encephalopathy. *Oncotarget*. 2016;7:78455–78472.
84. Lin W, Harding HP, Ron D, Popko B. Endoplasmic reticulum stress modulates the response of myelinating oligodendrocytes to the immune cytokine interferon-gamma. *J Cell Biol*. 2005;169:603–612.
85. Yatomi Y, Tanaka R, Shimada Y, et al. Type 2 diabetes reduces the proliferation and survival of oligodendrocyte progenitor cells in ischemic white matter lesions. *Neuroscience*. 2015; 289:214–223.
86. Iannitti T, Palmieri B. Clinical and experimental applications of sodium phenylbutyrate. *Drugs R D*. 2011;11:227–249.
87. Schonthal AH. Endoplasmic reticulum stress: its role in disease and novel prospects for therapy. *Scientifica (Cairo)*. 2012;2012:857516.
88. Smith W, Diaz GA, Lichter-Konecki U, et al. Ammonia control in children ages 2 months through 5 years with urea cycle disorders: comparison of sodium phenylbutyrate and glycerol phenylbutyrate. *J Pediatr*. 2013;162:1228–1234.
89. Jiang M, Liu L, He X, et al. Regulation of PERK-eIF2alpha signalling by tuberous sclerosis complex-1 controls homoeostasis and survival of myelinating oligodendrocytes. *Nat Commun*. 2016;7:12185.
90. Cahill H, Nathans J. The optokinetic reflex as a tool for quantitative analyses of nervous system function in mice: application to genetic and drug-induced variation. *PLoS One*. 2008;3:e2055.
91. Kretschmer F, Kretschmer V, Kunze VP, Kretzberg J. OMR-arena: automated measurement and stimulation system to determine mouse visual thresholds based on optomotor responses. *PLoS One*. 2013;8:e78058.
92. Ridder WH III, Nusinowitz S. The visual evoked potential in the mouse–origins and response characteristics. *Vision Res*. 2006;46:902–913.

Investigative Ophthalmology & Visual Science